

Random Walks with Tweedie: A Unified Framework for Diffusion Models

Chicago Y. Park[†], Michael T. McCann[‡], Cristina Garcia-Cardona[‡],
Brendt Wohlberg[‡], and Ulugbek S. Kamilov[†]

[†]Washington University in St. Louis, [‡]Los Alamos National Laboratory
{chicago, kamilov}@wustl.edu,
{mccann, cgarcia, brendt}@lanl.gov

Abstract

We present a simple template for designing generative diffusion model algorithms based on an interpretation of diffusion sampling as a sequence of random walks. Score-based diffusion models are widely used to generate high-quality images. Diffusion models have also been shown to yield state-of-the-art performance in many inverse problems. While these algorithms are often surprisingly simple, the theory behind them is not, and multiple complex theoretical justifications exist in the literature. Here, we provide a simple and largely self-contained theoretical justification for score-based-diffusion models that avoids using the theory of Markov chains or reverse diffusion, instead centering the theory of random walks and Tweedie’s formula. This approach leads to unified algorithmic templates for network training and sampling. In particular, these templates cleanly separate training from sampling, e.g., the noise schedule used during training need not match the one used during sampling. We show that several existing diffusion models correspond to particular choices within this template and demonstrate that other, more straightforward algorithmic choices lead to effective diffusion models. The proposed framework has the added benefit of enabling conditional sampling without any likelihood approximation.

1 Introduction

Deep score-based diffusion models are a type of generative model that uses a deep neural network to learn a score function—the gradient of the logarithm of a probability density—from training data. This score function is then used in an iterative algorithm based on the mathematical theory of diffusion to generate novel samples. These models (see [1] for a recent survey) have produced state-of-the-art results in generating natural images [2], videos [3], and 3D objects [4]. These algorithms have also been adapted to generate samples conditioned on noisy measurements, enabling their use for solving inverse problems (see [5] for a recent survey).

The success of diffusion models has led to the development of many training and sampling algorithms rooted in distinct mathematical theories. Although many of these algorithms have a similar structure, the specifics of the algorithm are often determined by the underlying theory, limiting its flexibility to accommodate different score functions and parameter configurations. Furthermore, conditional sampling often necessitates costly, problem-specific score training or relies on approximated posterior sampling.

The main aim of this work is to present a simple theoretical framework within which the distinctions between different diffusion model algorithms arise as algorithmic choices rather than as essential features of the underlying mathematical theory. This unified view is a step towards identifying the essential components of a diffusion model and determining how these differences contribute to algorithm performance. Our main contribution is a unified algorithmic template for diffusion models that includes widely-used algorithms such as the score-based generative model (SGM) [6], denoising diffusion probabilistic model (DDPM) [7], and score-based generative modeling through stochastic differential equations (Score-SDE) [8] as special cases. This framework is mathematically justified and flexible, e.g., it allows the noise schedule during training to differ from the one used during sampling and is compatible with pretrained denoisers (both variance-exploding and variance-preserving ones). Finally, the framework enables conditional sampling and Bayesian

Table 1: Proposed templates and parameter settings for common diffusion model algorithms, including the score-based generative model (SGM) [6], variance-exploding (VE) and variance-preserving (VP) diffusion models in SDE [8], and the denoising diffusion probabilistic model (DDPM) [7]. The templates unify algorithmic configurations for network training (specifying the noise scale distribution σ , the weight function $w(\sigma)$, and the denoising network r_θ), and sampling (specifying the noise level σ_k , step size τ_k , and temperature parameter \mathcal{T}_k). See Section 3 for details.

	Training template			Sampling template		
	$\mathcal{L}(\theta) = \mathbb{E}_{\sigma, \mathbf{X}, \mathbf{N}} [w(\sigma) \ \mathbf{X} - r_\theta(\mathbf{X} + \sigma \mathbf{N}, \sigma)\ _2^2], \quad \mathbf{X} \sim f_{\mathbf{X}}$			$\mathbf{x}_{k+1} = \mathbf{x}_k + \frac{\tau_k}{\sigma_k^2} (r_\theta(\mathbf{x}_k, \sigma_k) - \mathbf{x}_k) + \sqrt{2\tau_k \mathcal{T}_k} \mathbf{N}$ $= \mathbf{x}_k + \tau_k \nabla \log f_{\mathbf{X}_{\sigma_k}}(\mathbf{x}_k) + \sqrt{2\tau_k \mathcal{T}_k} \mathbf{N}$		
	σ	$w(\sigma)$	$r_\theta(\mathbf{x}, \sigma)$	σ_k	τ_k	\mathcal{T}_k
SGM	$\sim \mathcal{U}([\sigma_{\min}, \sigma_{\max}])$	σ^{-4}	$\mathbf{x} + \sigma^2 \mathbf{s}_\theta(\mathbf{x}, \sigma)$	σ_k	$\frac{\varepsilon \sigma_k^2}{2\sigma_{\max}^2}$	1
VE-SDE					$\sigma_k^2 - \sigma_{k+1}^2$	1/2
DDPM	$\sqrt{\frac{1-\bar{\alpha}_t}{\bar{\alpha}_t}}, t \sim \mathcal{U}(\{1, 2, \dots, T\})$	σ^{-2}	$\mathbf{x} - \sigma \epsilon_\theta(\sqrt{\bar{\alpha}_t(\sigma)} \mathbf{x}, t(\sigma))$	$\sqrt{\frac{1-\bar{\alpha}_{T-k}}{\bar{\alpha}_{T-k}}}$	$\frac{1-\alpha_{T-k}}{\bar{\alpha}_{T-k}}$	$\frac{\sigma_{T-k}^2 \alpha_{T-k}}{2-2\alpha_{T-k}}$
VP-SDE						

image reconstruction without any likelihood approximation. The implementation of our proposed method is publicly available.¹

None of the components of the proposed template or the supporting theory are new. For each component, we have aimed to both provide standard textbook references and pointers to appearances of similar ideas in the recent diffusion model literature.

1.1 Related Work

The most popular theoretical foundations for diffusion models are SGM [6], DDPM [7], and Score-SDE [8]. All these approaches train denoising score functions that operate on noisy data at varying noise levels. The SGM operates by gradually adding Gaussian noise to data and training a noise-conditional deep neural network to estimate the scores (or gradients) of the noisy data distributions, then generates new samples by using these estimated scores at progressively decreasing noise levels. On the other hand, DDPM uses two probabilistic Markov chains: a forward chain that gradually adds noise to the data, transforming it into a simple prior distribution (typically a standard Gaussian), and a reverse chain that learns to invert this process. During sampling, the reverse chain uses the learned denoising score function to remove noise step by step, following the same noise schedule as in the training process. Score-SDE extends the concepts of both SGM and DDPM to scenarios with an infinite number of time steps or noise levels. It uses stochastic differential equations (SDEs) to describe noise perturbation as forward SDEs and sample from target distribution by solving the corresponding reverse-time SDE using the learned score function. Although Score-SDE proposes a generalized framework of SGM and DDPM, it still requires corresponding denoisers for SGM-based and Markov-chain-based reverse process, respectively.

There exist several theoretical approaches for using diffusion models in conditional settings to solve inverse problems. Two common strategies are often employed to infer an unknown signal from degraded measurements using diffusion models: (a) training the conditional diffusion model on degraded measurements, allowing it to directly learn how to map from a known distribution (typically a standard Gaussian) to the desired quality signals, and (b) using a pretrained unconditional diffusion model and performing conditional sampling, incorporating an additional data consistency step during the sampling process. Strategy (a) can directly learn the posterior distribution of the desired signal given degraded measurement, but training task-specific diffusion models is data and computationally expensive process [9–11]. On the other hand, strategy (b) solves the inverse problem without requiring task-specific training by leveraging a pretrained unconditional diffusion model, but existing algorithms require some form of approximation because of intractable likelihood from multiple noise scales. One approach implements coarse-to-fine gradient ascent on the noisy distribution

¹https://github.com/wustl-cig/randomwalk_diffusion

by approximating the score from the residual between the output of a blind denoiser and the noisy input image [12]. Another approach [8, 13–16] suggests alternating between sampling steps and data consistency projections. A more recent approach [17–21] focuses on approximating the intractable time-dependent log-likelihood to achieve posterior sampling. Another line of work [22] sets only one noise level to allow the diffusion model to be used in Bayesian image reconstruction without additional likelihood approximation.

Building on the success of diffusion models in both unconditional generation and solving inverse problems, various theoretical frameworks have been proposed to understand and extend these models. Commonly used sampling strategies of diffusion models result in slightly different training and sampling algorithms, summarized in Table 1. Several works aim to establish the foundational theory of diffusion sampling. For instance, Score-SDE [8] proposes a generalized interpretation of noise perturbation and sampling processes to continuous-time processes using SDEs. The mathematical equivalence between time-inhomogeneous discrete-time diffusion models and time-homogeneous continuous-time Ornstein–Uhlenbeck processes evaluated at non-uniformly distributed observation times has been demonstrated [23]. The connection between diffusion models and Bayesian image reconstruction under a single noise level has been explored [22]. Furthermore, a unified framework for sampling and training in score-based diffusion models has been proposed [24], which defines a generalized marginal distribution for the latent variable with user-specific scaling for the mean and noise variance, as well as adjustable noise variance. Using this marginal distribution, a forward ODE is derived, showing how variance-exploding (VE) SDE and variance-preserving (VP) SDE can be viewed as instances of different choices of these scaling terms and noise variance for sampling. For training, a preconditioning framework is separately defined to identify the necessary scaling terms for the score’s input/output and the state variable across different diffusion models. Then, the noise distribution and the loss function’s weight constant are specified as key components of the training template. Note that our approach to proposing a unified template is distinct. We present a sampling template based on the interpretation of diffusion sampling as a sequence of random walks. Then, we show that existing foundational diffusion sampling methods are specific instances under more intuitive choices, such as step size, noise level, and a randomness control term. For the training template, we simplify the preconditioning step by incorporating minimum mean square error (MMSE) estimation along with the loss function’s weight constant and noise distribution in the training template.

2 Theory of Deep Score-Based Diffusion Sampling

We now present our theoretical justification for deep score-based generative modeling. While these results are not new (in fact, we have intentionally relied on textbook results), when brought together they offer a simple and mathematically rigorous justification for many diffusion model algorithms.

2.1 Tweedie’s formula

The score function—as the gradient of the log-likelihood—guides the denoising process in diffusion sampling, leading noisy data toward areas of higher probability density for image sampling. Tweedie’s formula [25] establishes a relationship between the score function and an optimal denoiser, offering an elegant approximation of the score using only the MMSE reconstruction and noisy images.

We denote a noisy version of a random variable, $\mathbf{X} \sim f_{\mathbf{X}}$, by

$$\mathbf{X}_\sigma = \mathbf{X} + \sigma \mathbf{N}, \quad \mathbf{N} \sim \mathcal{N}(\mathbf{0}, \mathbf{I}), \quad (1)$$

where σ is the specified noise level, and \mathbf{N} is a standard Gaussian sample.

MMSE image reconstruction recovers the image that, on average, is the closest to the ground truth given the observed measurements

$$\hat{\mathbf{x}}_{\text{MMSE}}(\mathbf{x}) = \arg \min_{\hat{\mathbf{x}}} \mathbb{E} [\|\hat{\mathbf{x}} - \mathbf{X}\|_2^2 \mid \mathbf{X}_\sigma = \mathbf{x}]. \quad (2)$$

With this, Tweedie’s formula establishes the relationship between score function and MMSE denoiser as

$$\nabla \log f_{\mathbf{X}_\sigma}(\mathbf{x}) = \frac{\hat{\mathbf{x}}_{\text{MMSE}}(\mathbf{x}) - \mathbf{x}}{\sigma^2}$$

for $\mathbf{x} \in \mathbb{R}^d$.

Note that $f_{\mathbf{X}_\sigma}$ is the noisy image distribution, which is distinct from the desired image distribution $f_{\mathbf{X}}$. Since the sum of random variables leads to a distribution that is the convolution of their individual distributions, $f_{\mathbf{X}_\sigma}$ is given by

$$f_{\mathbf{X}_\sigma}(\mathbf{x}) = \int_{\mathbb{R}^d} f_{\mathbf{X}}(\mathbf{x}') \phi_\sigma(\mathbf{x}' - \mathbf{x}) d\mathbf{x}',$$

where $\phi_\sigma(\cdot)$ is the probability density function of \mathbf{N} . Thus, we can view $f_{\mathbf{X}_\sigma}$ as a smoothed version of $f_{\mathbf{X}}$, and we can see from (1) that $\nabla \log f_{\mathbf{X}_\sigma} \rightarrow \nabla \log f_{\mathbf{X}}$ as $\sigma \rightarrow 0$.

2.2 CNN denoisers as MMSE estimators

Tweedie’s formula relates score functions with MMSE denoisers; we now show that neural networks trained on a denoising objective approximate MMSE denoisers. Consider the denoising inverse problem, where, as above, $\mathbf{X}_\sigma = \mathbf{X} + \sigma\mathbf{N}$ is a random variable representing \mathbf{X} perturbed by Gaussian noise with variance σ^2 , and denote the corresponding MMSE denoiser by $\hat{\mathbf{x}}_{\text{MMSE}} : \mathbb{R}^d \rightarrow \mathbb{R}^d$.

Given a set of IID training samples, $\mathbf{X}^{(1)}, \mathbf{X}^{(2)}, \dots, \mathbf{X}^{(N)} \sim f_{\mathbf{X}}$, we form noisy versions according to $\mathbf{X}_\sigma^{(n)} = \mathbf{X}^{(n)} + \sigma\mathbf{N}$. Then the mean squared error (MSE) loss for a reconstruction algorithm, $\hat{\mathbf{x}} : \mathbb{R}^d \rightarrow \mathbb{R}^d$, is

$$\begin{aligned} L(\hat{\mathbf{x}}) &= \frac{1}{N} \sum_{n=1}^N \|\hat{\mathbf{x}}(\mathbf{X}_\sigma^{(n)}) - \mathbf{X}^{(n)}\|_2^2 \\ &\approx \mathbb{E} [\|\hat{\mathbf{x}}(\mathbf{X}_\sigma) - \mathbf{X}\|_2^2]. \end{aligned} \tag{3}$$

The best possible reconstruction algorithm according to the average MSE metric is exactly the MMSE estimator (2) because

$$\hat{\mathbf{x}}_{\text{MMSE}}(\mathbf{x}) = \arg \min_{\hat{\mathbf{x}}} \mathbb{E} [\|\hat{\mathbf{x}} - \mathbf{X}\|_2^2 \mid \mathbf{X}_\sigma = \mathbf{x}] \tag{4a}$$

$$= \arg \min_{\hat{\mathbf{x}}} \int \|\hat{\mathbf{x}} - \mathbf{x}'\|_2^2 f_{\mathbf{X}|\mathbf{X}_\sigma}(\mathbf{x}'|\mathbf{x}) d\mathbf{x}' \tag{4b}$$

$$= \arg \min_{\hat{\mathbf{x}}} \int \|\hat{\mathbf{x}} - \mathbf{x}'\|_2^2 \frac{f_{\mathbf{X}, \mathbf{X}_\sigma}(\mathbf{x}', \mathbf{x})}{f_{\mathbf{X}_\sigma}(\mathbf{x})} d\mathbf{x}' \tag{4c}$$

$$= \arg \min_{\hat{\mathbf{x}}} \int \|\hat{\mathbf{x}} - \mathbf{x}'\|_2^2 f_{\mathbf{X}, \mathbf{X}_\sigma}(\mathbf{x}', \mathbf{x}) d\mathbf{x}', \tag{4d}$$

which implies that

$$\int \|\hat{\mathbf{x}}_{\text{MMSE}}(\mathbf{x}) - \mathbf{x}'\|_2^2 f_{\mathbf{X}, \mathbf{X}_\sigma}(\mathbf{x}', \mathbf{x}) d\mathbf{x}' \leq \int \|\hat{\mathbf{x}}(\mathbf{x}) - \mathbf{x}'\|_2^2 f_{\mathbf{X}, \mathbf{X}_\sigma}(\mathbf{x}', \mathbf{x}) d\mathbf{x}'$$

for any reconstruction algorithm $\hat{\mathbf{x}}$ and noisy image $\mathbf{X}_\sigma = \mathbf{x}$. Consequently,

$$\mathbb{E}(\|\hat{\mathbf{x}}_{\text{MMSE}}(\mathbf{X}_\sigma) - \mathbf{X}\|_2^2) \leq \mathbb{E}(\|\hat{\mathbf{x}}(\mathbf{X}_\sigma) - \mathbf{X}\|_2^2)$$

for all $\hat{\mathbf{x}}$. This implies that, within the limit of an infinitely large test set, the MMSE image reconstruction algorithm, by definition, achieves the lowest average MSE among all possible algorithms.

Thus, a well-trained deep denoiser r_θ —optimized to minimize the loss function in (3)—can serve as an accurate approximation of the MMSE estimator. The score then can be derived from this pretrained CNN denoiser using Tweedie’s formula

$$\nabla \log f_{\mathbf{X}_\sigma}(\mathbf{x}) = \frac{r_\theta(\mathbf{x}) - \mathbf{x}}{\sigma^2}.$$

These ideas have appeared in [26], which proposed estimating the score through denoising, based on the principle that the gradient of the log density at a noisy sample \mathbf{X}_σ naturally points toward the noise-free sample \mathbf{X} .

2.3 Random walk in a potential and the score function

Building on textbook results from stochastic differential equation theory, we show that simulating a particular random walk allows us to sample a PDF while only having access to the corresponding score function.

The motion (in d dimensions) of a particle influenced by Brownian motion and a potential V can be described by the equation

$$d\mathbf{X}_t = -\nabla V(\mathbf{X}_t)dt + \sqrt{2\mathcal{T}}d\mathbf{W}_t, \quad (5)$$

where \mathbf{X}_t is a random variable that represents the position of the particle at time t , $V: \mathbb{R}^d \rightarrow \mathbb{R}^d$ represents a potential, \mathbf{W}_t denotes standard Brownian motion on \mathbb{R}^d , $\mathcal{T} > 0$ is the temperature parameter controlling the extent of the random fluctuations, and \mathbf{X}_0 can be initialized either as a deterministic value or as a random variable following a specified probability density, such as a Gaussian distribution [27, Section 3.5, pg. 73].

For a fixed temperature $\mathcal{T} > 0$, if V grows fast enough that the particle cannot escape to infinity (see [27, Definition 4.2] for the technical condition) then for any distribution $f_{\mathbf{X}_0}$ of initial positions, the distribution

$$f_{\mathcal{T}}(\mathbf{x}) = \frac{1}{Z} e^{-\frac{V(\mathbf{x})}{\mathcal{T}}},$$

where

$$Z = \int_{\mathbb{R}^d} e^{-\frac{V(\mathbf{x})}{\mathcal{T}}} d\mathbf{x}$$

is the unique invariant distribution corresponding to (5) [27, Proposition 4.2]. This means that

$$\lim_{t \rightarrow \infty} f_{\mathbf{X}_t} = f_{\mathcal{T}}(\mathbf{x}).$$

As a first step towards our goal of drawing samples from a target distribution $f_{\mathbf{X}}$, we choose the potential

$$V(\mathbf{x}) = -\log f_{\mathbf{X}}(\mathbf{x}).$$

Equation (5) can then be discretized using the Euler-Maruyama method [27, Section 5.2, pg. 146] as follows:

$$\mathbf{x}_{k+1} = \mathbf{x}_k + \tau_k \nabla \log f_{\mathbf{X}}(\mathbf{x}_k) + \sqrt{2\tau_k \mathcal{T}_k} \zeta_k \quad k = 0, 1, 2, \dots$$

where $\nabla \log f_{\mathbf{X}}(\mathbf{x}_k)$ is the score function, τ_k denotes the step size at iteration k , and $\zeta_k \sim \mathcal{N}(\mathbf{0}, \mathbf{I})$.

A similar concept underpins the sampling approach in [6], where it is referred to as Langevin dynamics.

2.4 Sequence of random walks

We have thus far shown (closely following [22]) how a trained score can be used to generate samples from a noisy distribution, \mathbf{X}_{σ} . We now depart from [22] and describe how σ can be decreased during sampling to draw samples from the target distribution. This requires two ingredients: (a) a new sampling scheme that comprises a sequence of random walks with different potential functions, and (b) a denoiser for every noise level that can approximate the gradient of the corresponding potential.

To arrive at the new sampling scheme, consider a sequence of K random walks with different potential functions,

$$d\mathbf{x}_t = \begin{cases} \nabla \log f_{\mathbf{X}_{\sigma_0}}(\mathbf{x}_t)dt + \sqrt{2\mathcal{T}_0}d\mathbf{W}_t & t \in [0, t_0) \\ \nabla \log f_{\mathbf{X}_{\sigma_1}}(\mathbf{x}_t)dt + \sqrt{2\mathcal{T}_1}d\mathbf{W}_t & t \in [t_0, t_1) \\ \vdots & \vdots \\ \nabla \log f_{\mathbf{X}_{\sigma_{K-1}}}(\mathbf{x}_t)dt + \sqrt{2\mathcal{T}_{K-1}}d\mathbf{W}_t & t \in [t_{K-2}, t_{K-1}) \end{cases} \quad (6)$$

where σ_k decreases from a large value at $k = 0$ to a small value at σ_{K-1} so that $f_{\mathbf{X}_{\sigma_{K-1}}} \approx f_{\mathbf{X}}$. (Taking $\sigma_{K-1} = 0$ is not feasible in this framework because it results in a division by zero in Tweedie's formula.) A version of this idea appeared in [6] under the name annealed Langevin dynamics.

We can obtain a numerical solution to (6) by running a sequence of numerical solvers, each initialized with the result of the previous one. If the number of potential functions, K , is large relative to the difference between σ_0 and σ_{K-1} , we expect each solver to converge very quickly because the solution of one SDE is very similar to the solution of the next. Taking this idea to its limit, we propose using a sequence of random walks algorithm, each taking only one step. Doing so leads to our proposed sampling template, which we describe in the next section.

3 Proposed Diffusion Model Templates

In summary, a diffusion model algorithm can be derived by following a training and sampling template. The training template is

$$\mathcal{L}(\theta) = \mathbb{E}_{\sigma, \mathbf{X}, \mathbf{X}_\sigma} [w(\sigma) \|\mathbf{X} - r_\theta(\mathbf{X}_\sigma, \sigma)\|_2^2], \quad (7)$$

where $w : \mathbb{R}_{\geq 0} \rightarrow \mathbb{R}_{\geq 0}$ is a (user-specified) weight function, $\mathbf{X} \sim f_{\mathbf{X}}$ is a draw from the target distribution, $\sigma \sim f_\sigma$ is a user-specified noise scale distribution, and $\mathbf{X}_\sigma = \mathbf{X} + \sigma \mathbf{N}$ is a noisy version of \mathbf{X} .

The sampling template is

$$\mathbf{x}_{k+1} = \mathbf{x}_k + \tau_k \nabla \log f_{\mathbf{X}_{\sigma_k}}(\mathbf{x}_k) + \sqrt{2\tau_k \mathcal{T}_k} \mathbf{N}, \quad k = 0, 1, \dots, K-1 \quad (8)$$

where the sequences $\{\sigma_k\}$, $\{\tau_k\}$, and $\{\mathcal{T}_k\}$ are algorithmic parameters that represent noise levels, step sizes, and temperatures, respectively. From a theoretical perspective, the choice of the initial value \mathbf{x}_0 is arbitrary, but practically, it should be similar to a sample from \mathbf{X}_{σ_0} because the network $r_\theta(\cdot, \sigma_0)$ was trained on these samples. The noise level σ_k should decrease towards zero as the iteration k approaches $K-1$. The step size τ_k controls the balance between numerical stability (increasing with smaller τ) and the number of steps required for good quality samples (decreasing with larger τ). The temperature sequence \mathcal{T}_k should end with $\mathcal{T}_{K-1} = 1$ for sampling to be mathematically correct; setting the temperature below one drives sampling towards high density regions, setting it larger than one promotes faster mixing.

Note that while we have used uppercase bold symbols to denote random variables so far, the \mathbf{x}_k 's in the sampling template are written in lowercase for consistency with existing formulations.

When training is performed with the training template, we can substitute the trained network for the score function,

$$\mathbf{x}_{k+1} = \mathbf{x}_k + \frac{\tau_k}{\sigma_k^2} (r_\theta(\mathbf{x}_k, \sigma_k) - \mathbf{x}_k) + \sqrt{2\tau_k \mathcal{T}_k} \mathbf{N}, \quad k = 0, 1, \dots, K-1, \quad (9)$$

or equivalently

$$\mathbf{x}_{k+1} = \left(1 - \frac{\tau_k}{\sigma_k^2}\right) \mathbf{x}_k + \left(\frac{\tau_k}{\sigma_k^2}\right) r_\theta(\mathbf{x}_k, \sigma_k) + \sqrt{2\tau_k \mathcal{T}_k} \mathbf{N}, \quad k = 0, 1, \dots, K-1.$$

The first form resembles a randomized gradient descent and provides the intuition that τ_k should be chosen to be small relative to σ_k^2 to keep the effective step size small. The second form, emphasizes that the iterates mix the current image \mathbf{x}_k with its denoised version $r_\theta(\mathbf{x}_k)$.

In the following sections, we describe how the sampling template may be used with pretrained denoisers and interpret several existing diffusion model algorithms in terms of our proposed templates.

3.1 Using pretrained denoisers

Our sampling template admits the use of pretrained denoisers, however, care must be taken to properly scale their inputs and outputs to conform to the template. One way to achieve this is to interpret the training procedure in terms of the training template (7). Doing so results in an expression for the denoiser in the template, r_θ , in terms of the pretrained denoiser and is immediately compatible with the denoiser form of the sampling template (9). This is the approach we take in Section 3.2. In other cases, it is easier to work in terms of the score function form than the pretrained denoiser when applying the score-based sampling template (8). We pursue this approach here.

In deep score-based diffusion sampling, VE and VP score functions (and denoising networks) are widely used. These score functions are defined by two different ways of adding noise. In the VE setting, which SGM and VE-SDE adopt, the

noise variance increases at each step, with more noise being added as the process progresses according to

$$\mathbf{X}_t^{\text{VE}} = \mathbf{X} + \sigma_t \mathbf{N}.$$

In the VP setting, which DDPM and VP-SDE adopt, the total variance of the data is kept constant throughout the noise addition,

$$\mathbf{X}_t^{\text{VP}} = \sqrt{\bar{\alpha}_t} \cdot \left(\mathbf{X} + \sqrt{\frac{1 - \bar{\alpha}_t}{\bar{\alpha}_t}} \cdot \mathbf{N} \right), \quad (10)$$

where $\bar{\alpha}_t = \prod_{s=1}^t \alpha_s$, with t range from 1 to T . Here, α_t is chosen to ensure that \mathbf{X}_0^{VP} follows the desired probability distribution and \mathbf{X}_T^{VP} follows a known distribution, such as a standard Gaussian.

Due to the constant scale term applied to the noise-free image \mathbf{X} in (10), the VE score cannot be directly substituted for the VP score, and vice versa. Consequently, existing sampling schemes require a specific form of denoiser for sampling, distinguishing the two scores above. However, VP noise perturbation shows the scaled relationship with VE noise perturbation as $\mathbf{X}_t^{\text{VE}} = (1/\sqrt{\bar{\alpha}_t})\mathbf{X}_t^{\text{VP}}$ when σ_t is defined as $\sigma_t = \sqrt{(1 - \bar{\alpha}_t)/\bar{\alpha}_t}$. For a probability density function scaled by different random variables, we can derive the gradient (i.e., score) relationship as follows. Given that

$$f_{\mathbf{X}_t^{\text{VE}}}(\mathbf{x}) = \sqrt{\bar{\alpha}_t} f_{\mathbf{X}_t^{\text{VP}}}(\sqrt{\bar{\alpha}_t} \mathbf{x}),$$

where $\mathbf{X}_t^{\text{VE}} = (1/\sqrt{\bar{\alpha}_t})\mathbf{X}_t^{\text{VP}}$ and $\sigma_t = \sqrt{(1 - \bar{\alpha}_t)/\bar{\alpha}_t}$, we proceed by taking the logarithm on both sides:

$$\log f_{\mathbf{X}_t^{\text{VE}}}(\mathbf{x}) = \log \sqrt{\bar{\alpha}_t} + \log f_{\mathbf{X}_t^{\text{VP}}}(\sqrt{\bar{\alpha}_t} \mathbf{x}).$$

Differentiating with respect to \mathbf{x} gives:

$$\nabla \log f_{\mathbf{X}_t^{\text{VE}}}(\mathbf{x}) = \sqrt{\bar{\alpha}_t} \nabla \log f_{\mathbf{X}_t^{\text{VP}}}(\sqrt{\bar{\alpha}_t} \mathbf{x}). \quad (11)$$

Comparing \mathbf{X}_t^{VE} with \mathbf{X}_σ in (1), we can derive:

$$\begin{aligned} \nabla \log f_{\mathbf{X}_\sigma}(\mathbf{x}) &= \nabla \log f_{\mathbf{X}_t^{\text{VE}}}(\mathbf{x}) \\ &= \sqrt{\bar{\alpha}_t} \nabla \log f_{\mathbf{X}_t^{\text{VP}}}(\sqrt{\bar{\alpha}_t} \mathbf{x}), \end{aligned}$$

where any score can be used adaptively within a single sampling template (8).

This score relationship also allows us to relate VE and VP scores via the MMSE reconstruction of the noise-free image r_θ :

$$\begin{aligned} r_\theta(\mathbf{x}_t) &= \mathbf{x}_t + \sigma_t^2 \nabla \log f_{\mathbf{X}_t^{\text{VE}}}(\mathbf{x}_t) \\ &= \mathbf{x}_t + \frac{1 - \bar{\alpha}_t}{\sqrt{\bar{\alpha}_t}} \nabla \log f_{\mathbf{X}_t^{\text{VP}}}(\sqrt{\bar{\alpha}_t} \mathbf{x}_t). \end{aligned}$$

3.2 Interpretation of Existing Methods

The VP training objective in our template. DDPM [7] and VP-SDE [8] use the same VP training objective. To represent this objective in terms of the training template (7), we set the noise variance distribution to

$$\sigma = \sqrt{\frac{1 - \bar{\alpha}_t}{\bar{\alpha}_t}} \quad t \sim \text{Uniform}(1, \dots, T), \quad (12)$$

with $\bar{\alpha}_t$ defined as in [7]. Doing this establishes bijections between t , σ , and $\bar{\alpha}$ because $\bar{\alpha}_t$ is monotone by definition. Let $w(\sigma) = \sigma^{-2}$. Let the denoiser r_θ take the form

$$r_\theta(\mathbf{x}, \sigma) = \mathbf{x} - \sigma \epsilon_\theta(\sqrt{\bar{\alpha}_{t(\sigma)}} \mathbf{x}, t(\sigma)), \quad (13)$$

where $t(\sigma)$ denotes the t that corresponds to a given sigma via (12) and ϵ_θ is defined as in [7].

Substituting these choices into the template loss, we have

$$(7) = \mathbb{E}_{\sigma, \mathbf{X}, \mathbf{X}_\sigma} [\sigma^{-2} \|\mathbf{X} - (\mathbf{X}_\sigma - \sigma \boldsymbol{\epsilon}_\theta(\sqrt{\bar{\alpha}_t(\sigma)} \mathbf{X}_\sigma, t(\sigma)))\|_2^2] \quad (14a)$$

$$= \mathbb{E}_{\sigma, \mathbf{X}, \mathbf{N}} [\sigma^{-2} \|\mathbf{X} - (\mathbf{X} + \sigma \mathbf{N} - \sigma \boldsymbol{\epsilon}_\theta(\sqrt{\bar{\alpha}_t(\sigma)} \mathbf{X} + \sqrt{\bar{\alpha}_t(\sigma)} \sigma \mathbf{N}, t(\sigma)))\|_2^2] \quad (14b)$$

$$= \mathbb{E}_{\sigma, \mathbf{X}, \mathbf{N}} [\|\mathbf{N} - \boldsymbol{\epsilon}_\theta(\sqrt{\bar{\alpha}_t(\sigma)} \mathbf{X} + \sqrt{\bar{\alpha}_t(\sigma)} \sigma \mathbf{N}, t(\sigma))\|_2^2] \quad (14c)$$

$$= \mathbb{E}_{t, \mathbf{X}, \mathbf{N}} [\|\mathbf{N} - \boldsymbol{\epsilon}_\theta(\sqrt{\bar{\alpha}_t} \mathbf{X} + \sqrt{\bar{\alpha}_t} \sigma \mathbf{N}, t)\|_2^2] \quad (14d)$$

$$= \mathbb{E}_{t, \mathbf{X}, \mathbf{N}} [\|\mathbf{N} - \boldsymbol{\epsilon}_\theta(\sqrt{\bar{\alpha}_t} \mathbf{X} + \sqrt{1 - \bar{\alpha}_t} \mathbf{N}, t)\|_2^2], \quad (14e)$$

which is the VP training loss [7, Algorithm 1 and (14)].

The VE training objective in our template. SGM [6] and VE-SDE [8] both use the same VE training objective. To represent this objective in terms of the training template (7): Let the distribution of noise scales by uniform selection over a set $\{\sigma_0, \sigma_1, \dots, \sigma_{L-1}\}$. Let the denoiser take the form

$$r_\theta(\mathbf{x}, \sigma) = \mathbf{x} + \sigma^2 \mathbf{s}_\theta(\mathbf{x}, \sigma),$$

where $\mathbf{s}_\theta(\mathbf{x}, \sigma)$ is the noise conditional score function as defined in [6]. Let $w(\sigma) = \sigma^{-4}$. Substituting these choices into the training template results in

$$(7) = \mathbb{E}_{\sigma, \mathbf{X}, \mathbf{X}_\sigma} [\sigma^{-4} \|\mathbf{X} - (\mathbf{X}_\sigma + \sigma^2 \mathbf{s}_\theta(\mathbf{X}_\sigma, \sigma))\|_2^2] \quad (15a)$$

$$= \mathbb{E}_{\sigma, \mathbf{X}, \mathbf{X}_\sigma} [\sigma^{-4} \|\sigma^2 \mathbf{s}_\theta(\mathbf{X}_\sigma, \sigma) + \mathbf{X}_\sigma - \mathbf{X}\|_2^2] \quad (15b)$$

$$= \mathbb{E}_{\sigma, \mathbf{X}, \mathbf{X}_\sigma} \left[\left\| \mathbf{s}_\theta(\mathbf{X}_\sigma, \sigma) + \frac{\mathbf{X}_\sigma - \mathbf{X}}{\sigma^2} \right\|_2^2 \right] \quad (15c)$$

$$\approx \frac{1}{L} \sum_{\ell=0}^{L-1} \mathbb{E}_{\mathbf{X}, \mathbf{X}_{\sigma_\ell}} \left[\lambda(\sigma_\ell) \left\| \mathbf{s}_\theta(\mathbf{X}_{\sigma_\ell}, \sigma_\ell) + \frac{\mathbf{X}_{\sigma_\ell} - \mathbf{X}}{\sigma_\ell^2} \right\|_2^2 \right], \quad (15d)$$

where $\lambda(\sigma_\ell) > 0$ is a user-specify coefficient function depending on σ_ℓ , and the derived form of training objective corresponds to the VE training loss [6, (5-6)].

DDPM sampling in our template. To prove that sampling iterate of DDPM [7] is a specific instance of our sampling template in (8), we begin with the sampling iterates from [7, Algorithm 2] and change variables to arrive at our sampling template. We start with

$$\mathbf{x}_{t-1} = \frac{1}{\sqrt{\alpha_t}} (\mathbf{x}_t - \frac{1 - \alpha_t}{\sqrt{1 - \alpha_t}} \boldsymbol{\epsilon}_\theta(\mathbf{x}_t, t)) + \sigma'_t \mathbf{N},$$

where σ'_t denotes the user-defined noise schedule from [7], which turns out to be distinct from the template noise schedule.

Replacing $\boldsymbol{\epsilon}_\theta(\mathbf{x}_t, t)$ with the score using Tweedie's formula [25]:

$$\boldsymbol{\epsilon}_\theta(\mathbf{x}_t, t) = -\sqrt{1 - \bar{\alpha}_t} \nabla \log f_{\mathbf{X}_{\bar{\alpha}_t}}(\mathbf{x}_t),$$

where $\mathbf{X}_{\bar{\alpha}_t}$ is equivalent to \mathbf{X}_t^{VP} in (10).

$$\mathbf{x}_{t-1} = \frac{1}{\sqrt{\alpha_t}} (\mathbf{x}_t + (1 - \alpha_t) \nabla \log f_{\mathbf{X}_{\bar{\alpha}_t}}(\mathbf{x}_t)) + \sigma'_t \mathbf{N}.$$

Letting $\mathbf{s}_t = \mathbf{x}_t / \sqrt{\bar{\alpha}_t}$, we have

$$\sqrt{\bar{\alpha}_{t-1}} \mathbf{s}_{t-1} = \frac{1}{\sqrt{\alpha_t}} (\sqrt{\bar{\alpha}_t} \mathbf{s}_t + (1 - \alpha_t) \nabla \log f_{\mathbf{X}_{\bar{\alpha}_t}}(\sqrt{\bar{\alpha}_t} \mathbf{s}_t)) + \sigma'_t \mathbf{N}$$

$$\mathbf{s}_{t-1} = \frac{1}{\sqrt{\alpha_t \bar{\alpha}_{t-1}}} (\sqrt{\bar{\alpha}_t} \mathbf{s}_t + (1 - \alpha_t) \nabla \log f_{\mathbf{X}_{\bar{\alpha}_t}}(\sqrt{\bar{\alpha}_t} \mathbf{s}_t)) + \frac{\sigma'_t}{\sqrt{\bar{\alpha}_{t-1}}} \mathbf{N},$$

where we remain the score’s random variable as $\mathbf{X}_{\bar{\alpha}_t}$, since this matches how the score is trained. And because [7] defines $\bar{\alpha}_t = \prod_{s=1}^t \alpha_s$, we have that $\alpha_t \bar{\alpha}_{t-1} = \bar{\alpha}_t$ and therefore

$$\mathbf{s}_{t-1} = \mathbf{s}_t + \frac{1 - \alpha_t}{\sqrt{\bar{\alpha}_t}} \nabla \log f_{\mathbf{X}_{\bar{\alpha}_t}}(\sqrt{\bar{\alpha}_t} \mathbf{s}_t) + \frac{\sqrt{\bar{\alpha}_t} \sigma'_t}{\sqrt{\bar{\alpha}_t}} \mathbf{N}.$$

We let $k = t$ so that iterations count up rather than down and assume a total number of iterations $K = T + 1$, following the contention in [7]. Additionally, we rename \mathbf{s} back to \mathbf{x} , and we use the score relationship in (11) to rewrite $\nabla \log f_{\mathbf{X}_{\bar{\alpha}_t}}$ in terms of $\nabla \log f_{\mathbf{X}_{\sigma_k}}$, where we define $\sigma_k = \sqrt{(1 - \bar{\alpha}_{T-k})/\bar{\alpha}_{T-k}}$. This leads to

$$\mathbf{x}_{k+1} = \mathbf{x}_k + \frac{1 - \alpha_{T-k}}{\bar{\alpha}_{T-k}} \nabla \log f_{\mathbf{X}_{\sigma_k}}(\mathbf{x}_k) + \frac{\sqrt{\alpha_{T-k}} \sigma'_{T-k}}{\sqrt{\bar{\alpha}_{T-k}}} \mathbf{N}.$$

We can then rearrange it to match the form of the sampling template (8)

$$\mathbf{x}_{k+1} = \mathbf{x}_k + \frac{1 - \alpha_{T-k}}{\bar{\alpha}_{T-k}} \nabla \log f_{\mathbf{X}_{\sigma_k}}(\mathbf{x}_k) + \sqrt{2 \left(\frac{1 - \alpha_{T-k}}{\bar{\alpha}_{T-k}} \right) \left(\frac{(\sigma'_{T-k})^2 \alpha_{T-k}}{2 - 2\alpha_{T-k}} \right)} \mathbf{N}.$$

In [7], two different choices for the sequence σ'_t are described, with both yielding similar results. Our analysis reveals that this sequence affects the temperature of the sampling and that the temperature needs to approach one in order correctly sample the target distribution. In the notation of [7], this requirement is $\frac{\sigma'^2_{T-k} \alpha_{T-k}}{2 - 2\alpha_{T-k}} \rightarrow 1$.

Note we omit the proof for the VP-SDE sampling since the predictor-based VP-SDE iterates from [8, Algorithm 3] are equivalent to the DDPM iterates by the proof in [8, Appendix E].

SGM sampling in our template. Since SGM corresponds to the same formulation as our template, replacing time step t with iteration k is all we need to match between our sampling template and sampling iterates from [6, Algorithm 1]:

$$\mathbf{x}_{k+1} = \mathbf{x}_k + \frac{\varepsilon \sigma_k^2}{2\sigma_{\max}^2} \nabla \log f_{\mathbf{X}_{\sigma_k}}(\mathbf{x}_k) + \sqrt{\frac{\varepsilon \sigma_k^2}{\sigma_{\max}^2}} \mathbf{N}$$

where σ_k is the designed noise level for the current state \mathbf{x}_k and lies between σ_{\min} and σ_{\max} , and ε is empirically found constant between 10^{-5} and 10^{-4} [6].

VE-SDE sampling in our template. Same as the matching proof of SGM, VE-SDE has exactly the same formulation as our template. So, we can replace the time step t with iteration k is all we need to match between our sampling template and sampling iterates from [8, Algorithm 2]:

$$\mathbf{x}_{k+1} = \mathbf{x}_k + (\sigma_k^2 - \sigma_{k+1}^2) \nabla \log f_{\mathbf{X}_{\sigma_k}}(\mathbf{x}_k) + \sqrt{\sigma_k^2 - \sigma_{k+1}^2} \mathbf{N}.$$

This demonstrates that our sequence of random walks framework further generalizes the Score-SDE. We also provide a straightforward instance of our template in Section 5.2 and 5.3, which can still sample plausible images.

4 Theory of Deep Score-Based Diffusion for Conditional Sampling

Building on our theoretical justification for deep score-based generative modeling, we extend this theory to conditional sampling. We provide the underlying theory and demonstrate that our sequence of random walks framework can be adapted for posterior sampling, offering the advantage of not requiring likelihood approximations, as is often needed in many existing methods.

4.1 Inverse problems

Solving inverse problems involves estimating an unknown image $\mathbf{x} \in \mathbb{R}^d$ from its noisy measurement $\mathbf{y} \in \mathbb{R}^d$. From a Bayesian perspective, this involves inferring the posterior distribution $f_{\mathbf{X}|\mathbf{Y}}(\mathbf{x} | \mathbf{y})$ from the learned prior distribution $f_{\mathbf{X}}(\mathbf{x})$ of the desired image by incorporating the likelihood term $f_{\mathbf{Y}|\mathbf{X}}(\mathbf{y} | \mathbf{x})$

$$f_{\mathbf{X}|\mathbf{Y}}(\mathbf{x} | \mathbf{y}) \propto f_{\mathbf{Y}|\mathbf{X}}(\mathbf{y} | \mathbf{x}) f_{\mathbf{X}}(\mathbf{x}), \quad (16)$$

where $f_{\mathbf{Y}|\mathbf{X}}(\mathbf{y} | \mathbf{x})$ is a conditional PDF that describes how the known imaging system relates the measurements \mathbf{y} to the unknown signal \mathbf{x} . This relationship involves incorporating the conditional score in the sampling process as $\nabla \log f_{\mathbf{X}_{\bar{\alpha}_{T-k}}|\mathbf{Y}}(\mathbf{x}_k | \mathbf{y}) = \nabla(\log f_{\mathbf{Y}|\mathbf{X}_{\bar{\alpha}_{T-k}}}(\mathbf{y} | \mathbf{x}_k) + \log f_{\mathbf{X}_{\bar{\alpha}_{T-k}}}(\mathbf{x}_k))$.

In practice, measurements \mathbf{y} are modeled as

$$\mathbf{y} = \mathbf{A}\mathbf{x} + \mathbf{e}, \quad \mathbf{e} \sim \mathcal{N}(\mathbf{0}, \eta^2 \mathbf{I}) \quad (17)$$

where \mathbf{A} is the degradation operator (also called forward operator), \mathbf{x} is the noise-free image, and \mathbf{e} is additive white Gaussian noise with measurement noise level η . Since \mathbf{y} is distributed according to $\mathcal{N}(\mathbf{A}\mathbf{x}, \mathbf{e})$, by the definition of normal distribution PDF, we can derive the log-likelihood gradient as

$$\nabla \log f_{\mathbf{Y}|\mathbf{X}}(\mathbf{y} | \mathbf{x}) = \frac{1}{\eta^2} \mathbf{A}^T (\mathbf{y} - \mathbf{A}\mathbf{x}). \quad (18)$$

However, for a noisy latent image \mathbf{x}_k during the diffusion process, \mathbf{y} is no longer distributed according to $\mathcal{N}(\mathbf{A}\mathbf{x}_k, \mathbf{e})$. As a result, computing the exact log-likelihood gradient $\nabla \log f_{\mathbf{Y}|\mathbf{X}_{\sigma_k}}(\mathbf{y} | \mathbf{x}_k)$ during the diffusion process remains a challenge. To address this, some existing works sample from posterior distribution by training a conditional model on degraded measurements, which allows direct approximation of $\nabla \log f_{\mathbf{X}_{\sigma_k}|\mathbf{Y}}(\mathbf{x}_k | \mathbf{y})$ [9–11]. However, as it requires problem-specific training, leveraging pretrained unconditional diffusion model with data consistency steps is an active research area. To approximate the intractable time-dependent log-likelihood, Ajil et al. [17] proposes

$$\nabla \log f_{\mathbf{Y}|\mathbf{X}_{\sigma_k}}(\mathbf{y} | \mathbf{x}_k) \approx \mathbf{A}^T \frac{\mathbf{A}\mathbf{x}_k - \mathbf{y}}{\eta^2 + (\gamma_k)^2},$$

where $(\gamma_k)^2$ is an annealing hyper-parameter. The class of denoising diffusion restoration models (DDRM) methods [18,19] adopts the approximation

$$\nabla \log f_{\mathbf{Y}|\mathbf{X}_{\sigma_k}}(\mathbf{y} | \mathbf{x}_k) \approx \frac{\mathbf{y} - \mathbf{x}_k}{|\eta^2 - (\sigma_k)^2|},$$

where σ_k denotes the noise level at diffusion iteration k , in the scenario where the degradation operator $\mathbf{A} = \mathbf{I}$ in (17). For a general \mathbf{A} , singular value decomposition is applied to weight the spectral components based on the noise level of each component. Diffusion posterior sampling (DPS) [20] proposes

$$\nabla \log f_{\mathbf{Y}|\mathbf{X}_{\sigma_k}}(\mathbf{y} | \mathbf{x}_k) \approx \nabla \log f_{\mathbf{Y}|\mathbf{X}_{\sigma_k}}(\mathbf{y} | r_\theta(\mathbf{x}_k, \sigma_k)),$$

where $r_\theta(\mathbf{x}_k, \sigma_k)$ is the MMSE reconstruction of noise-free image \mathbf{x}_0 given an input of \mathbf{x}_k and noise level σ_k (see [5] for more comprehensive survey). The important point from the observation of existing algorithms is that those algorithms require the approximation of the log-likelihood gradient. At the end of the next section, we extend our sequence of random walks framework to solve inverse problems without any likelihood approximation.

4.2 Sequence of random walks to solve inverse problems

In Section 3, we introduce the sequence of random walks framework as sampling template of existing diffusion algorithms. Our theory of the sequence of random walks can easily be modified to enable sampling from a posterior distribution, thereby providing a way to solve inverse problems with a learned prior. In addition, our framework has the added benefit of enabling conditional sampling without any likelihood approximation.

As described in Section 4.1, for conditional sampling, we replace log-prior gradient $\nabla \log f_{\mathbf{X}_{\sigma_k}}(\mathbf{x}_k)$ with log-posterior gradient $\nabla \log f_{\mathbf{X}_{\sigma_k}|\mathbf{Y}}(\mathbf{x}_k | \mathbf{y})$ in unconditional sequence of random walks.

$$\begin{aligned} \mathbf{x}_{k+1} &= \mathbf{x}_k + \tau_k \nabla \log f_{\mathbf{X}_{\sigma_k}|\mathbf{Y}}(\mathbf{x}_k | \mathbf{y}) + \sqrt{2\tau_k \mathcal{T}_k} \mathbf{N} \\ &= \mathbf{x}_k + \tau_k \left(\nabla \log f_{\mathbf{X}_{\sigma_k}}(\mathbf{x}_k) + \frac{1}{\eta^2} \mathbf{A}^T (\mathbf{y} - \mathbf{A}\mathbf{x}_k) \right) + \sqrt{2\tau_k \mathcal{T}_k} \mathbf{N} \end{aligned}$$

where η is the measurement noise level. Note that our conditional sequence of random walks framework does not require any measurement consistency projection step or approximation of log-likelihood. The logic behind it is that as $k \rightarrow \infty$ and $\tau_k \rightarrow 0$, the iteration converges to the distributions $f_{\mathbf{X}}$ and $f_{\mathbf{Y}|\mathbf{X}}$.

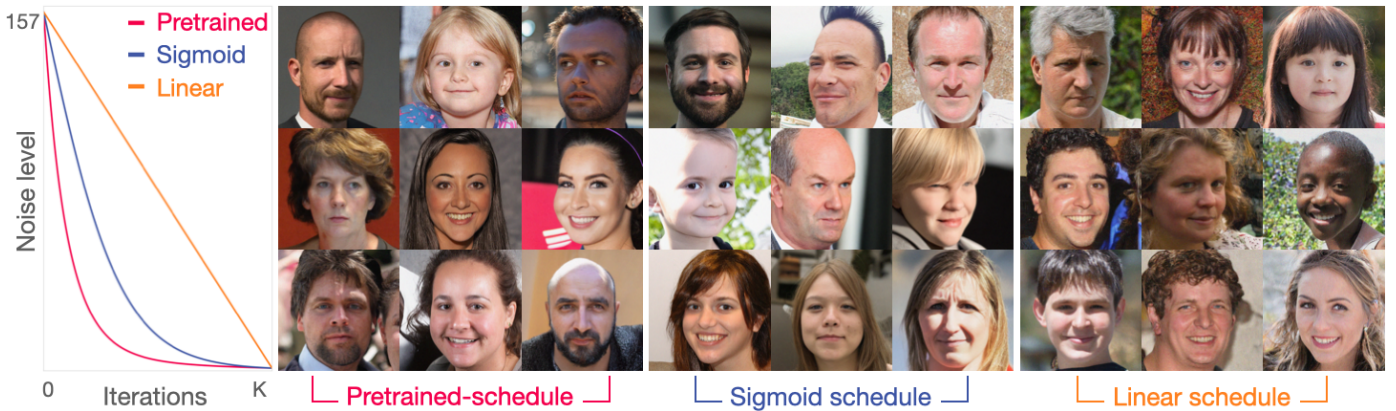


Figure 1: Unconditional image generation with VP-score-based sequence of random walks under different noise scheduling schemes. In contrast to existing score-based diffusion sampling algorithms, which require the sampling iterations to strictly follow the noise scheduling scheme of the pretrained score function due to dependence on the Markov chain, this figure demonstrates that our framework can fully decouple from the training process by allowing $\bar{\alpha}_t$ to be defined from arbitrary noise levels σ_t , such as those following sigmoid or linear schedules.

For the internal parameter setup, the Lipschitz constant L of the likelihood term $\nabla \log f_{Y|X_{\sigma_k}}(\mathbf{y}|\mathbf{x}_k)$ can be defined based on the forward measurement operator. We then ensure that the step size range is $\tau_k \leq 1/L$ to meet the known requirements for convergence.

5 Demonstration of proposed theory

While the main contribution of this work is the simple theoretical justification and unified template for diffusion model algorithms presented in Section 2 and 3, we now demonstrate concrete implementations of the theory. In particular, we show unconditional generation using arbitrarily defined simple noise schedules and straightforward parameter specifications in a sequence of random walks framework. We empirically show this generalized and simplified approach can also be applicable to conditional generation with the added benefit of eliminating the need for any approximation of the gradient of log-likelihood.

We now describe our experimental setup, including dataset and pretrained networks, and experiment results of our sequence of random walks framework.

5.1 Dataset and pretrained neural networks

For numerical validation, we use two distinct types of pretrained diffusion models, both trained on the FFHQ 256×256 face dataset [28]. For the VP diffusion model, we use the one from DPS [20], which follows the VP training template in Table 1 with a linear schedule for α ranging from $\alpha_0 = 0.9999$ to $\alpha_T = 0.98$. We also adapt a pretrained VE diffusion model from Score-SDE [8], which follows the VE training template in Table 1 with the noise level σ varies from $\sigma_0 = 348$ to $\sigma_K = 0.01$. To validate the unconditional sampling capability of our framework, we demonstrate that any type of denoiser can be used in our single framework. Also, we demonstrate that our framework can generate images with arbitrary schedule sigmoid and linear, independent of the denoiser’s training scheme.

5.2 Unconditional image sampling with straightforward parameter choice of sequence of random walks

In Section 3, we showed that both the Markov chain theory in DDPM [7] and the reverse SDE theory in Score-SDE [8] can be viewed as making particular choices of step sizes τ_k and temperature parameters \mathcal{T}_k in our framework in (8). In



Figure 2: Unconditional image generation with VE-score-based sequence of random walks. This figure illustrates the flexibility of our sequence of random walks framework, which enables unconditional sampling with the VE score while also being compatible with the VP score under a unified framework. This implies that our framework can use any type of score without restricting the score training scheme.

this section, we show that alternative, straightforward parameter choices can provide similar unconditional sampling results.

We propose a straightforward scheme for specifying the step size and temperature term. We define step size as a noise-level-dependent value based on the intuition that the step size should be small relative to the noise level in the current latent image \mathbf{x}_k . Specifically, we set $\tau_k = \varepsilon \sigma_k^2$, where ε is a constant scaling factor. Based on the theory in Section 2.3, we simplify temperature selection by setting \mathcal{T}_0 and linearly progressing to $\mathcal{T}_{K-1} = 1$ as the final value. This allows us to write the simplified instance within our sampling template as follows:

$$\begin{aligned} \mathbf{x}_{k+1} &= \mathbf{x}_k + \varepsilon \cdot (\sigma_k)^2 \cdot \nabla \log f_{\mathbf{x}_{\sigma_k}}(\mathbf{x}_k) + \sqrt{2 \cdot \varepsilon \cdot (\sigma_k)^2 \mathcal{T}_k} \mathbf{N} \\ &= \mathbf{x}_k + \varepsilon \cdot (\sigma_k)^2 \cdot \sqrt{\bar{\alpha}_k} \cdot \nabla \log f_{\mathbf{x}_{\bar{\alpha}_k}}(\sqrt{\bar{\alpha}_k} \cdot \mathbf{x}_k) + \sqrt{2 \cdot \varepsilon \cdot (\sigma_k)^2 \mathcal{T}_k} \mathbf{N}, \end{aligned}$$

where $\sigma_k = \sqrt{(1 - \bar{\alpha}_k)/\bar{\alpha}_k}$, with $\{\sigma_k\}_{k=0}^{K-1}$ being a given sequence that implicitly determines $\bar{\alpha}_k$.

Under the proposed simplified scheme, we compare three different choices for the noise level σ_k in τ_k and $\nabla \log f_{\mathbf{x}_{\sigma_k}}$. In the first, which we call **Pretrained-schedule**, we set $\{\sigma_k\}_{k=0}^{K-1}$ to follow the same noise schedule used during the training of the pretrained score function, as outlined in Table 1. In the second, which we call **sigmoid**, we set $\{\sigma_k\}_{k=0}^{K-1}$ following the specification from [29, second setup in Figure 3 (c)], matching only the initial and final noise levels to the pretrained score function’s noise sequence. In the third, which we call **linear**, we set $\{\sigma_k\}_{k=0}^{K-1}$ as the straight line connecting the maximum and minimum levels of the pretrained score function’s noise sequence. Note that the second and third schemes are entirely independent of the intermediate noise schedule of the pretrained score function, demonstrating flexibility in designing a sampling formulation using the score function across the trained noise range, without requiring adherence to a specific noise schedule for all steps. To specify the ε in τ_k , since it remains constant throughout the iterations, their values can be easily adjusted empirically, simplifying the tuning process.

Given the time-conditional VP score functions rather than noise-level conditional VE score functions, we need to find the appropriate time for the VP score to match an arbitrary noise level at each iteration. To achieve this, we introduce a noise-to-time mapping function $t(\sigma_k)$. Given $\{\bar{\alpha}_t\}_{t=1}^T$ based on the scheduling of the pretrained VP score functions, we derive the noise sequence of VP networks as $\{\sqrt{(1 - \bar{\alpha}_t)/\bar{\alpha}_t}\}_{t=1}^T$ as outlined in Section 3.1. First, this function linearly interpolates $\{\sqrt{(1 - \bar{\alpha}_t)/\bar{\alpha}_t}\}_{t=1}^T$ over the range $[1, 2, \dots, K']$, where K' can be much larger than number of iterations

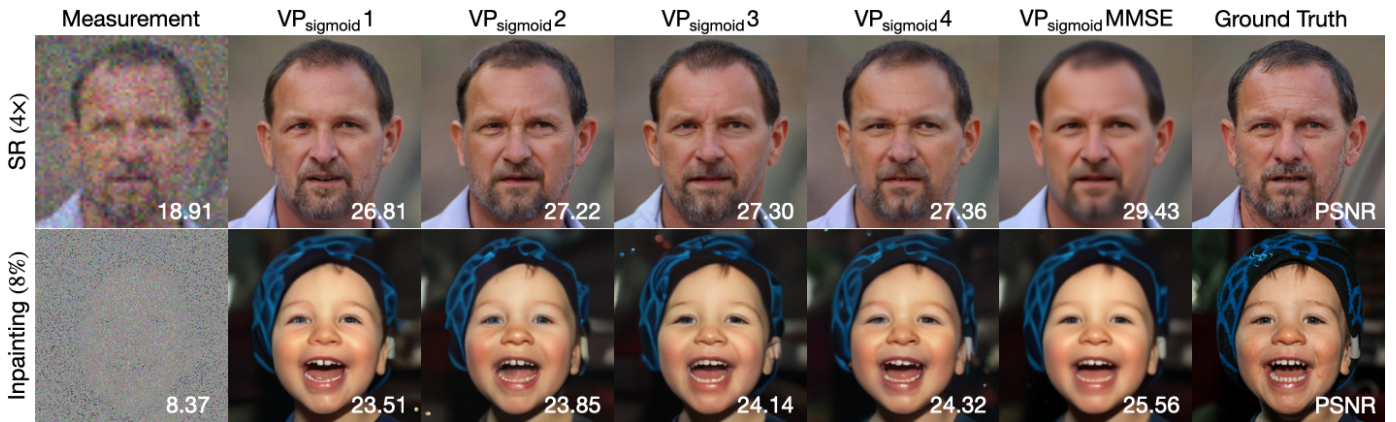


Figure 3: Conditional image sampling results with the VP-score-based sequence of random walks with sigmoid noise scheduling. We conditionally sample four images under the same setup, and $VP_{\text{sigmoid}}\text{MMSE}$ represents the pixel-wise average of 500 samples. The figure illustrates that our simplified framework can extend beyond unconditional image synthesis to effectively solve inverse problems.

K for precise matching. This function then finds $t' = \arg \min_{t' \in [1, K']} |\sigma_k - \sqrt{(1 - \bar{\alpha}_{t'}) / \bar{\alpha}_{t'}}|$ and returns $T(\frac{t'}{K'})$ as a conditional time input of the VP score function.

For image generation using the VP diffusion model, we take 10,000 iterations for the denoiser and sigmoid schedules and 150,000 iterations for the linear schedule. For each noise schedule, we specify the parameters as follows: for the pretrained schedule, $(\mathcal{T}_0 = 0.85, \varepsilon_{\text{pretrained}} = 0.08)$; for the sigmoid schedule, $(\mathcal{T}_0 = 0.85, \varepsilon_{\text{sigmoid}} = 0.06)$; and for the linear schedule, $(\mathcal{T}_0 = 0.95, \varepsilon_{\text{linear}} = 0.08)$. To sample images using the VE diffusion model, we take 10,000 iterations and set $(\mathcal{T}_0 = 0.6, \varepsilon_{\text{pretrained}} = 0.02)$. We did not include the sigmoid and linear version of the VE diffusion model because of redundancy with the VP experiment result.

Figures 1 and 2 illustrate that the proposed simplified sequence of random walks framework can generate plausible images with any type of denoiser, and for VP-score-based sequence of random walks, it shows that arbitrary noise scheduling can define noise level in the step size τ_k instead of exactly referring pretrained score function’s noise schedule.

5.3 Solving inverse problems using sequence of random walks

We demonstrate the conditional sampling capability of our framework on two inverse problems. For **random inpainting**, the forward operator corresponds to randomly masking out 92% of the total pixels (across all RGB channels). For **super-resolution**, the forward operator is bicubic downsampling by a factor of 4. For both problems, we set measurement noise $\eta = 0.2$. We took $K = 10,000$ sampling steps and set step size $\tau_k = \min(\varepsilon \cdot (\sigma_k)^2, \eta^2)$ which ensures our step size is smaller than the Lipschitz constant of log-likelihood term. We performed sampling with both the pretrained VP and VE networks as described in Section 5.1. To sample via the VP network, we used the sigmoid noise schedule from Section 5.2 and specified the remaining parameters as follows: for super-resolution $(\mathcal{T}_0 = 1, \varepsilon_{\text{sigmoid}} = 0.22)$ and for inpainting $(\mathcal{T}_0 = 1, \varepsilon_{\text{sigmoid}} = 0.38)$. For the VE network, we specified parameters as $(\mathcal{T}_0 = 1, \varepsilon_{\text{pretrained}} = 0.05)$ for both inverse problems.

Figure 3 shows results for sampling with the VP network. The four conditional samples look plausible as faces and correspond well to the measurements. We also computed the pixel-wise average of 500 samples. For each of these, we computed the PSNR with respect to the ground truth according to

$$\text{PSNR}(\mathbf{x}) = 10 \log_{10} \left(\frac{1}{\text{MSE}(\mathbf{x}_{\text{ground truth}}, \mathbf{x})} \right). \quad (19)$$

Training images were scaled between 0 and 1 for the VE score and between -1 and 1 for the VP score. Sample images from the VP network were rescaled to lie between 0 and 1. No clipping was applied to either score function, allowing all

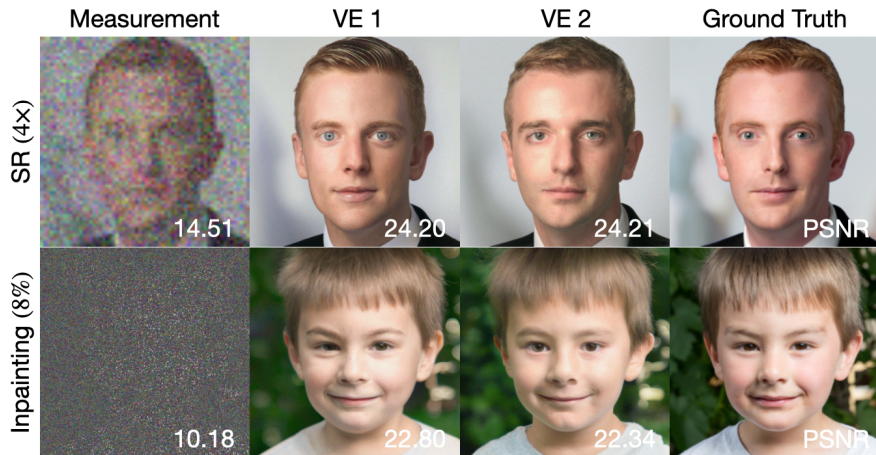


Figure 4: Conditional sampling result with VE-score-based sequence of random walks to solve super-resolution and random inpainting. It demonstrates that the interchangeability of the VP and VE scores extends to solving inverse problems beyond unconditional image synthesis.

sampled values to be retained. The PSNRs for the samples were lower than for the average result, which makes sense because the average result should be an approximation of the MMSE reconstruction, which maximizes PSNR on average. Figure 4 shows that the VE diffusion model also applies to our framework to solve inverse problems.

6 Conclusion

We have introduced a simple and self-contained theoretical justification for score-based diffusion models that interprets sampling as solving a sequence of stochastic differential equations. This approach provides an algorithmic template that encompasses a variety of algorithms from the literature, including SGM [6], DDPM [7], and Score-SDE [8]. The advantages of our work are that (a) it provides a unified interpretation of existing score-based sampling algorithms; (b) it simplifies score-based generation by decoupling the sampling noise schedule from the training noise schedule, removing the need to define forward and reverse stochastic processes; (c) it provides algorithms for conditional sampling (i.e., solving inverse problems) without any log-likelihood approximation. While we do not claim a new state-of-the-art for generative modeling, we empirically demonstrate that a simple parameter and noise schedule selection within this framework can generate high-quality unconditional and conditional images.

Viewing diffusion models as we do here provides fertile ground for future work. We believe it will be particularly valuable to compare different noise schedules and weightings in the training template and develop efficient methods for tuning the step size and temperature parameters during sampling. We hope that these explorations will reveal diffusion model algorithms that are easy to train and efficiently generate high-quality, diverse samples.

References

- [1] Ryan Po, Wang Yifan, Vladislav Golyanik, Kfir Aberman, Jonathan T. Barron, Amit Bermano, Eric Chan, et al., “State of the art on diffusion models for visual computing,” in *Computer Graphics Forum*, 2024, vol. 43, p. e15063.
- [2] Prafulla Dhariwal and Alexander Nichol, “Diffusion models beat GANs on image synthesis,” in *Advances in Neural Information Processing Systems*, 2021, vol. 34, pp. 8780–8794.
- [3] Jonathan Ho, Tim Salimans, Alexey Gritsenko, William Chan, Mohammad Norouzi, and David J. Fleet, “Video diffusion models,” in *Advances in Neural Information Processing Systems*, 2022, vol. 35, pp. 8633–8646.

- [4] Biao Zhang, Jiapeng Tang, Matthias Niessner, and Peter Wonka, “3dshape2vecset: A 3d shape representation for neural fields and generative diffusion models,” *ACM Transactions on Graphics (TOG)*, vol. 42, no. 4, pp. 1–16, 2023.
- [5] Hyungjin Chung, Hyelin Nam, and Jong Chul Ye, “Review of diffusion models: Theory and applications,” *Journal of the Korean Society for Industrial and Applied Mathematics*, vol. 28, no. 1, pp. 1–21, 2024.
- [6] Yang Song and Stefano Ermon, “Generative modeling by estimating gradients of the data distribution,” in *Advances in Neural Information Processing Systems*, 2019, vol. 32.
- [7] Jonathan Ho, Ajay Jain, and Pieter Abbeel, “Denoising diffusion probabilistic models,” in *Advances in Neural Information Processing Systems*, 2020, vol. 33, pp. 6840–6851.
- [8] Yang Song, Jascha Sohl-Dickstein, Diederik P. Kingma, Abhishek Kumar, Stefano Ermon, and Ben Poole, “Score-based generative modeling through stochastic differential equations,” in *9th International Conference on Learning Representations (ICLR)*, 2021.
- [9] Jay Whang, Mauricio Delbracio, Hossein Talebi, Chitwan Saharia, Alexandros G. Dimakis, and Peyman Milanfar, “Deblurring via stochastic refinement,” in *Proceedings of the IEEE/CVF Conference on Computer Vision and Pattern Recognition*, 2022, pp. 16293–16303.
- [10] Chitwan Saharia, Jonathan Ho, William Chan, Tim Salimans, David J. Fleet, and Mohammad Norouzi, “Image super-resolution via iterative refinement,” *IEEE Transactions on Pattern Analysis and Machine Intelligence*, vol. 45, no. 4, pp. 4713–4726, 2022.
- [11] Jiaming Liu, Rushil Anirudh, Jayaraman J. Thiagarajan, Stewart He, K. Aditya Mohan, Ulugbek S. Kamilov, and Hyojin Kim, “DOLCE: A model-based probabilistic diffusion framework for limited-angle CT reconstruction,” in *Proceedings of the IEEE/CVF International Conference on Computer Vision*, 2023, pp. 10498–10508.
- [12] Zahra Kadkhodaie and Eero Simoncelli, “Stochastic solutions for linear inverse problems using the prior implicit in a denoiser,” in *Advances in Neural Information Processing Systems*, 2021, vol. 34, pp. 13242–13254.
- [13] Zahra Kadkhodaie and Eero P. Simoncelli, “Stochastic solutions for linear inverse problems using the prior implicit in a denoiser,” in *Advances in Neural Information Processing Systems*, A. Beygelzimer, Y. Dauphin, P. Liang, and J. Wortman Vaughan, Eds., 2021.
- [14] Hyungjin Chung, Byeongsu Sim, and Jong Chul Ye, “Come-closer-diffuse-faster: Accelerating conditional diffusion models for inverse problems through stochastic contraction,” in *Proceedings of the IEEE/CVF Conference on Computer Vision and Pattern Recognition*, 2022, pp. 12413–12422.
- [15] Hyungjin Chung and Jong Chul Ye, “Score-based diffusion models for accelerated MRI,” *Medical Image Analysis*, p. 102479, 2022.
- [16] Yang Song, Liyue Shen, Lei Xing, and Stefano Ermon, “Solving inverse problems in medical imaging with score-based generative models,” in *International Conference on Learning Representations*, 2022.
- [17] Ajil Jalal, Marius Arvinte, Giannis Daras, Eric Price, Alexandros G. Dimakis, and Jon Tamir, “Robust compressed sensing MRI with deep generative priors,” in *Advances in Neural Information Processing Systems*, 2021, vol. 34, pp. 14938–14954.
- [18] Bahjat Kawar, Gregory Vaksman, and Michael Elad, “Stochastic image denoising by sampling from the posterior distribution,” in *Proceedings of the IEEE/CVF International Conference on Computer Vision (ICCV) Workshops*, 2021, pp. 1866–1875.
- [19] Bahjat Kawar, Michael Elad, Stefano Ermon, and Jiaming Song, “Denoising diffusion restoration models,” in *Advances in Neural Information Processing Systems*, 2022, vol. 35, pp. 23593–23606.

- [20] Hyungjin Chung, Jeongsol Kim, Michael Thompson McCann, Marc Louis Klasky, and Jong Chul Ye, “Diffusion posterior sampling for general noisy inverse problems,” in *The Eleventh International Conference on Learning Representations*, 2023.
- [21] Jiaming Song, Arash Vahdat, Morteza Mardani, and Jan Kautz, “Pseudoinverse-guided diffusion models for inverse problems,” in *International Conference on Learning Representations*, 2023.
- [22] Michael T. McCann, Hyungjin Chung, Jong Chul Ye, and Marc L. Klasky, “Score-based diffusion models for bayesian image reconstruction,” in *2023 IEEE International Conference on Image Processing (ICIP)*, 2023, pp. 111–115.
- [23] Javier E. Santos and Yen Ting Lin, “Using Ornstein-Uhlenbeck process to understand denoising diffusion probabilistic model and its noise schedules,” *arXiv preprint arXiv:2311.17673*, 2023.
- [24] Tero Karras, Miika Aittala, Timo Aila, and Samuli Laine, “Elucidating the design space of diffusion-based generative models,” in *Advances in Neural Information Processing Systems*, 2022, vol. 35, pp. 26565–26577.
- [25] Bradley Efron, “Tweedie’s formula and selection bias,” *Journal of the American Statistical Association*, vol. 106, no. 496, pp. 1602–1614, 2011.
- [26] Pascal Vincent, “A connection between score matching and denoising autoencoders,” *Neural Computation*, vol. 23, no. 7, pp. 1661–1674, 2011.
- [27] Grigorios A. Pavliotis, *Stochastic processes and applications*, vol. 60 of *Texts in Applied Mathematics*, Springer, 2014.
- [28] Tero Karras, Samuli Laine, and Timo Aila, “A style-based generator architecture for generative adversarial networks,” in *Proceedings of the IEEE/CVF Conference on Computer Vision and Pattern Recognition*, 2019, pp. 4401–4410.
- [29] Ting Chen, “On the importance of noise scheduling for diffusion models,” *arXiv preprint arXiv:2301.10972*, 2023.